Laser Chem. 1983, Vol. 3, pp. 57–72
0278-6273/83/0306-0057$12.00/0

Printed in Great Britain

Electronic Energy Partitioning in Photodissociation

SHERWIN J. SINGER and KARL F. FREED†

The Department of Chemistry and The James Franck Institute, The University of Chicago, Chicago, Illinois 60637

YEHUDA B. BAND‡

Ben Gurion University of the Negev, Beer Sheva, Israel, and Allied Corporation, 7 Powder-Horn Drive, Mt. Bethel, N.J. 07060

Despite the apparent simplicity of photodissociation in diatomic molecules, some of the essential physics of this process is not understood when there is fine structure in the atomic photofragments. Previous theories cannot treat the branching ratios and angular distributions of the individual fine structure sublevels. We have developed a complete quantum mechanical theory of the effects of nonadiabatic couplings and of electronic angular momentum on the fine structure branching ratios, angular distributions, and polarization in diatomic photodissociation. When the photofragments separate with large relative kinetic energy, simple limiting expressions can be obtained for branching ratios and the symmetry parameters which characterize fragment angular distributions and polarized fluorescence from excited fragments. Information about the symmetry of the molecular states involved in the optical transition which dissociates the molecule may be deduced from fine structure branching ratios and asymmetry parameters in the high energy limit. At low relative kinetic energies where non-adiabatic couplings are crucial, cross sections and asymmetry parameters exhibit interesting behavior which intimately reflect the shape of the dissociative molecular surfaces. We employ the example of sodium hydride photodissociation to produce ^{2}P excited sodium atoms as a model system because of the availability of *ab initio* potential curves and oscillator strength matrix elements. The low energy photodissociation cross section and angular distributions are shown to exhibit resonances which arise in part due to non-adiabatic spin–orbit and Coriolis couplings. Their energy dependence can therefore be utilized to probe the nature of potential curves which are not directly pumped in optical absorption processes and may therefore provide a unique spectroscopic means for measuring properties of these "dark" states.

† Research supported, in part, by NSF Grant Che 80-23456.
‡ Research supported, in part, by the US–Israel Binational Science Foundation.

1. INTRODUCTION

One of the important decay channels of excited molecular states involves decomposition. Molecular dissociation processes play a vital role in many chemical systems that are fundamental to the description of chemical reactions, of atmospheric processes, and astrophysical and biological problems. There has been great interest recently in understanding how the energy content of an excited molecule prior to dissociation is partitioned among available photofragment degrees of freedom. Significant progress from both the experimental and theoretical viewpoint has been made in determining the distribution of the total energy of the excited molecule among fragment translational, rotational, and vibrational degrees of freedom when the dissociation may be assumed to proceed on a single electronic potential energy surface. (For recent reviews, see Refs. 1–4.) In contrast, the partitioning of the energy of the excited molecule among electronic degrees of freedom of the photofragments has not received much attention. However, it is necessary to understand electronic energy partitioning in order to predict the response of photofragments to various experimental probes and to maximize the information which may be extracted from experimental data. For instance, one of the most useful experimental probes of photodissociation dynamics, absorption and emission of polarized light by photofragments, is very sensitive to the fragment electronic state distribution.

In this paper we study diatomic molecule photodissociation when more than one fragment electronic state is energetically accessible and, consequently, the dissociation involves motion on more than one electronic surface. Transitions between electronic states induced by non-adiabatic interactions occur as the fragments separate and affect the distribution of fragment electronic states. The nascent superposition of electronic states produced immediately after absorption of a photon is altered, often quite drastically, by electronically non-adiabatic coupling. Treatment of electronic energy partitioning in diatomic molecule photodissociation is important because the effect of non-adiabatic interactions is significant whenever the photofragments have non-vanishing angular momentum. Also, study of diatomic dissociation in the presence of non-adiabatic coupling is a first step toward understanding electronic energy partitioning in polyatomic molecule dissociation.

Electronically non-adiabatic interactions always play a crucial role in photodissociation dynamics near a threshold for dissociation when the fragments possess non-vanishing electronic angular momentum.[5,6] For diatomic molecules, non-adiabatic interactions need to be considered unless the dissociation leaves both fragments in ^1S electronic states. The role of non-adiabatic interactions is common and not confined to traditionally studied examples in which two electronic potential energy surfaces cross or nearly cross. We provide a full quantum theory for dissociation of light atom diatomics in another publication.[7] In this paper we present an introduction to the theory which explains the strong influence of non-adiabatic interactions upon molecular dissociation and highlight the effects of non-adiabatic coupling that may be observed experimentally.

Non-adiabatic interactions near a dissociation threshold provide a mechanism which may be exploited to great advantage to increase the information about excited molecular potential energy curves gained from a photodissociation experiment. In the course of the dissociation, non-adiabatic couplings cause transitions to molecular electronic states which otherwise would not participate in the dissociation dynamics, making these "dark" states accessible to experimental investigation. Inclusion of non-adiabatic interactions is essential in the calculation of photodissociation transition amplitudes to fragment internal states produced by photodissociation. These amplitudes characterize a coherent superposition of final fragment states which may be probed using various experimental techniques. We have derived[7] theoretical expressions for the following observables which are often measured in the laboratory:

1) cross sections to fine structure levels of atomic fragments.

2) photofragment angular distributions for each fine structure level.

3) cross sections for fluorescence emitted by excited fragments in various fine structure states with arbitrary direction of propogation and polarization. (Similar considerations also apply to absorption of polarized light by photofragments and are applicable to detection of fragments by laser induced fluorescence techniques.)

4) joint cross sections for the simultaneous angular resolution of photofragments and polarized fluorescence (or absorption of polarized light).

For each observable cross section given above, we have derived expressions suitable for single photon dissociation and for two-photon, two-color dissociation.[7] The latter process is advantageous because the first photon allows for selection of the rotational, vibrational and electronic state of the diatom prior to excitation to the dissociative surface. Our investigations to date are confined to photodissociation of diatomics, although the theoretical methods we describe can be extended to larger molecules.

In Section 2 we explain the physical motivation for the theory and the reasons why non-adiabatic interactions are important in many cases where they have been overlooked so far. Section 3 contains a description of analytic approximations for various differential cross sections which are valid when the relative translational energy available to the photofragments is much greater than the magnitude of the non-adiabatic couplings. In many cases this high energy approximation allows prediction of the photofragment angular distributions and polarization of fluorescence emitted by excited fragments based solely upon the symmetry of the molecular states involved in the optical excitation of the molecule and without the need for any dynamical calculations. At lower translational energies numerical calculations are necessary to generate cross sections for detailed comparison with experimental data. In Section 4 we present results of recent calculations for dissociation of NaH to $Na(^2P_{1/2,3/2})$ and $H(^2S_{1/2})$[8] to illustrate the detailed information available in the dependence of various cross sections on the preparation of the molecule, the energy available to the dissociating molecule, and the fine structure state of the fragments.

2. PHYSICAL MOTIVATION OF THE THEORY

We consider dissociation of a diatom to light atoms which can be described by L–S coupling. The treatment of other coupling cases follows similarly. Throughout this paper, the subscripts a and b refer to the two atomic fragments. The various atomic term limits are denoted by c_a and c_b. The first three atomic term limits (thresholds for dissociation) for the a–b molecule are shown in Figure 1. At small internuclear separations, the molecular region, the interaction between the two atoms is dominated by forces arising from

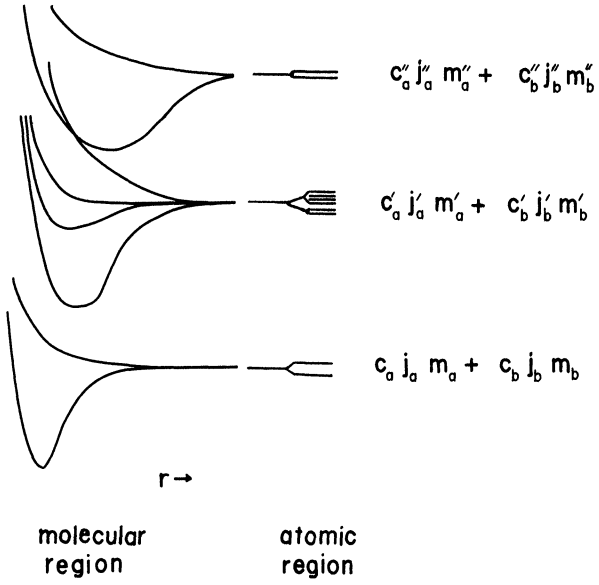

FIGURE 1 Schematic representation of molecular electronic potential surfaces and their atomic term limits. The internuclear separation is r. The levels of each atomic term limit are split by spin–orbit interaction. A possible curve crossing in the molecular region is indicated.

interaction among all the electrons and nuclei, including exchange interactions.

To lowest order, the full wave function for both the initial bound state and excited states in the molecular region is a product of wave functions for radial motion of the nuclei, rotation of the symmetry axis of the diatom with respect to a space fixed (SF) coordinate system, and an adiabatic Born–Oppenheimer (ABO) electronic wave function,

$$\Psi_{(\text{molecular basis})} = \psi_{EJMc\Lambda S\Sigma}(r) D^{J*}_{M\Omega}(\alpha\beta\gamma)|c\,\Lambda S\Sigma\rangle \qquad (2.1)$$

For purposes of illustration, a Hund's case (a) wave function is given above, where $D^{J*}_{M\Omega}(\alpha\beta\gamma)$ is a Wigner rotation matrix element and $(\alpha\beta\gamma)$ are the Euler angles which rotate the SF coordinate system into a body fixed (BF) coordinate system in which the symmetry axis of the diatom is along the BF z-axis. The interfragment separation is r; the total spin quantum number is S; Λ and Σ are the projections of electronic orbital and spin angular momentum, respectively; and

M is the projection of total angular momentum J on the SF z-axis. The relative magnitudes of the rotational constant relative to the fine structure splitting determines whether a Hund's case (a) or case (b) wave function is more appropriate for light atoms. The analysis is readily considered using any Hund's case wave function.

Non-adiabatic couplings arise from various terms in the full diatomic molecule Hamiltonian. For instance, the Coriolis interaction couples states in which the projection Ω of total angular momentum differs by one unit. Spin–orbit coupling mixes states which may differ in S, Λ, and Σ, but not in Ω. The radial derivative in the nuclear kinetic energy operator acts on the ABO electronic wave function to couple molecular states with the same quantum numbers Λ, S, and Σ. Therefore the exact total wave function in the molecular region actually is a linear combination of the molecular states of (2.1). However, in the absence of curve crossings, the ABO electronic energy eigenvalues are usually well separated in this region, and the effect of non-adiabatic couplings may be taken into account with perturbation theory.

Several molecular potential energy curves converge to one atomic term limit if the atomic fragments have non-vanishing electronic angular momentum (Figure 1). We refer to the asymptotic region at large internuclear separations as the atomic region. In the atomic region, the approximate molecular states (2.1) are still coupled by non-adiabatic interactions. Coriolis couplings, which are proportional to r^{-2}, vanish slowly at large r and spin–orbit coupling between molecular states persists to all interfragment separations. However, the approximate molecular states that correlate at large interfragment separations with the same atomic limit become energetically degenerate at large r, and the non-adiabatic coupling between them can no longer be treated perturbatively. Instead, we expand the wave function in the atomic region in products of wave functions for radial nuclear motion, orbital motion of the nuclei about the center of mass, and atomic fine structure states for each of the fragments.

$$\Psi^{(\text{atomic basis})} \underset{r\to\infty}{\longrightarrow} \sum_{lmc_a j_a m_a c_b j_b m_b} \psi_{lmc_a j_a m_a c_b j_b m_b}(r)\, Y_{lm}(\hat{\mathbf{r}})|c_a j_a m_a\rangle|c_b j_b m_b\rangle \qquad (2.2)$$

In the above equation j_a and m_a (j_b and m_b) are the quantum numbers for total electronic angular momentum and projection along the SF

z-axis which label the atomic fine structure states of fragment a (b). The Y_{lm} ($\hat{\mathbf{r}}$) are spherical harmonics and $\hat{\mathbf{r}}$ is a unit vector along the internuclear axis in the SF coordinate system. In general, the molecular states (2.1) are strongly coupled at large interfragment separations and do not form a proper basis for expansion of the wave function in the atomic region. Therefore, it is only meaningful to calculate photodissociation transition amplitudes to the atomic fragment states (2.2), and not to the molecular states (2.1).

As the molecule dissociates, the interplay between the forces which dominate in the molecular region and those which dominate in the atomic region determines the final superposition of fragment eigenstates. This superposition is strongly influenced by the energy available to the dissociating molecule, the rotational, vibrational, and electronic state of the initial complex, and the molecular potential energy curves. At photon energies near threshold for dissociation, we predict the following behavior to be observed:

1) non-statistical branching ratios to fine structure states of the same atomic term limit which vary as a function of photon energy.

2) angular distributions of photofragments which change dramatically across the threshold region. Different fine structure states have different angular distributions.

3) photodissociation cross sections, angular distributions, and polarized fluorescence from excited atomic fragments reflect a wealth of resonance phenomena near the dissociation threshold. Resonance phenomena are also predicted to appear as a result of molecular states normally not considered in the dissociation dynamics (for instance, triplet states if the initial molecular state before excitation is a singlet).

The threshold phenomena described above are all exhibited in our calculations for NaH which are discussed in Section 4. Similar phenomena are predicted for the photodissociation of other diatomic molecules.

As the photon energy increases the fragments eventually recede from each other with translational energy much larger than the magnitude of the non-adiabatic couplings. In this high energy regime, the transition amplitudes often tend to limiting values which are independent of the photon energy. This high energy limit, often called the recoil limit,[9] is described in the following section.

3. HIGH ENERGY LIMIT

At high translational energies the wave function for motion on the dissociative surfaces change diabatically from the molecular to the atomic regime as discussed in Section 2 above. In another article[7] we show that in the limit of large translational energy, or the recoil limit, the dissociation dynamics may be broken into two steps which may be treated separately: First the molecule is excited from the initial state to a dissociative electronic surface. Transitions between electronic states in the molecular region can be neglected at high translational energies except for special cases where curve crossings occur. Secondly, the dynamical effect of non-adiabatic coupling is realized at the boundary of the molecular and atomic regions by matching a wave function given by a sum of molecular states (2.1) to the asymptotic atomic form (2.2) at the boundary surface. In the recoil limit the transition amplitude $\tau(lmj_am_aj_bm_b|i)$ from an initial state indicated by the index i to the fragment eigenstate labelled by quantum numbers l, m, j_a, m_a, j_b, and m_b is given by a sum of products of molecular transition amplitudes $\tau(c\Lambda S\Sigma|i)$ and orthogonal transformation elements which transform the large r limit of the molecular states (2.1) into the atomic eigenstates (2.2)

$$\tau(lmc_aj_am_ac_bj_bm_b|i) = \sum_{c\Lambda S\Sigma} \tau(c\Lambda S\Sigma|i)\langle c\Lambda S\Sigma|lmc_aj_am_ac_bj_bm_b\rangle \qquad (3.1)$$

The transition amplitude $\tau(c\Lambda S\Sigma|i)$ depends on the magnitude of the oscillator strength from the initial state to a particular molecular state while the transformation element $\langle c\Lambda S\Sigma|lmc_aj_am_ac_bj_bm_b\rangle$ accounts for the sudden switch from molecular to atomic regimes.

The transformation elements on the right hand side of (3.1) are analytically given in terms of angular momentum recoupling coefficients.[7] When only one dissociative molecular state carries oscillator strength from the ground state, the sum on the right-hand side of (3.1) may be omitted. In this case the magnitude of $\tau(c\Lambda S\Sigma|i)$ cancels when various asymmetry parameters for fragment angular distributions, polarized fluorescence, etc., which are actually ratios of partial cross sections, are calculated. These asymmetry parameters then have fixed numerical values independent of the oscillator strength from the ground state and therefore independent of photon energy. Consequently, when only one molecular state participates in the

dissociation, the recoil limit asymmetry parameters are given by analytic, although complicated, sums over standard angular momentum recoupling coefficients.[7] If more than one dissociative molecular state carries oscillator strength from the ground state, the contribution from each dissociative state must be included as given in (3.1). The latter case leads to the persistence of interference effects between different excited molecular states at high translational energies.

In Table I we present the degree of polarization of fluorescence emitted by an excited photofragment for several common atomic term limits and molecular transitions in the recoil limit. In these examples we assume a Hund's case (a) diatom is dissociated by a single photon of linearly polarized light and fluorescence in each example is produced by decay of the P-state fragment to an S-state. The general formula is given elsewhere.[7] The polarization ratio P is defined by

$$P = \frac{I_{\parallel} - I_{\perp}}{I_{\parallel} + I_{\perp}} \tag{3.2}$$

TABLE I
Polarization ratio in axial recoil limit as a function of initial, intermediate, and final quantum numbers

Atomic limit	Molecular transition	Fine structure level of P-state fragment	Polarization ratio of fluorescence from $P \rightarrow S$ state transition
$^1P+{}^1S$	$^1\Sigma \rightarrow {}^1\Sigma$	1	1/2
	$^1\Sigma \rightarrow {}^1\Pi$	1	7/9
	$^1\Pi \rightarrow {}^1\Sigma$	1	−1/3
	$^1\Pi \rightarrow {}^1\Pi$	1	−1/3
$^2P+{}^2S$	$^1\Sigma \rightarrow {}^1\Pi$	3/2	21/47
$^3P+{}^2S$	$^2\Sigma \rightarrow {}^2\Sigma$	1	1/7
		2	21/107
	$^2\Sigma \rightarrow {}^2\Pi$	1	21/87
		2	143/449
	$^2\Pi_{1/2} \rightarrow {}^2\Pi$	1	−3/19
		2	21/107
	$^2\Pi_{3/2} \rightarrow {}^2\Pi$	1	1/7
		2	−21/93

where $I_{\parallel}$ and $I_{\perp}$ are the intensities of spontaneously emitted light polarized parallel and perpendicularly, respectively, to the polarization vector of the initial excitation. Note that the predicted polarization varies with fine structure level in the case of fluorescence from a ^3P level where more than one fine structure level can give rise to polarized fluorescence. (Spontaneously emitted light from fine structure state $|j, m\rangle$ is completely unpolarized if $j < 1$.) Also, note that, in general, different molecular transitions which correlate with the same atomic limit give rise to different polarizations. Excitation from different multiplet components of the initial electronic state can influence the polarization of fluorescence from fragment fine structure level, as shown in the case of $^2\Pi_{1/2,3/2} \rightarrow {}^2\Pi$ excitation. *In summary, the pattern of polarized fluorescence from atomic fragment fine structure levels provides a "fingerprint" which points to the symmetry and multiplet component of the molecular states involved in the optical excitation of the diatom.*

Our analytical recoil limit calculations predict non-statistical branching ratios in certain cases even at high translational energies. The relative cross sections to the three fine structure states of the ^3P limit produced by $^2\Pi_{1/2,3/2} \rightarrow {}^2\Pi$ excitation are shown in Table II. The relative cross sections for the $j = 0, 1, 2$ fine structure states are different depending on the initial multiplet from which the molecule is excited and are *not* in a 1 : 3 : 5 statistical ratio. However, the sum of cross sections over initial multiplet states *is* statistical. We are able to prove[7] that averaging over initial multiplet levels always results in a statistical branching ratio if, for instance, one of the fragments is in an S-state. Therefore, dissociation of diatoms in a thermal distribu-

TABLE II

Branching ratio to fragment fine structure levels in axial recoil limit as a function of initial multiplet level: $^2\Pi_{1/2,3/2} \rightarrow {}^2\Pi$ molecular transition

Molecular transition	Relative cross section to fine structure levels of P fragment		
	$^3P_0$	$^3P_1$	$^3P_2$
$^2\Pi_{1/2} \rightarrow {}^2\Pi$	1	9/4	5/4
$^2\Pi_{3/2} \rightarrow {}^2\Pi$	0	3/4	15/4
Sum of $^2\Pi_{1/2} \rightarrow {}^2\Pi$ and $^2\Pi_{3/2} \rightarrow {}^2\Pi$	1	3	5

tion of multiplet states does not result in non-statistical branching ratios, at least if one fragment is in an S-state. However, if the molecule can be prepared in a single multiplet components, say, by the first photon in a two-photon, two-color, dissociation, then our results suggest that non-statistical branching ratios may be observed, even in the recoil limit.

4. EXACT QUANTUM CALCULATIONS

We report results of exact close coupled calculations for the dissociation of NaH to $Na(^2P_{1/2,3/2}) + H(^2S_{1/2})$. The ground state of NaH is an $X\ ^1\Sigma^+$electronic state. The dissociative surfaces that correlate at large interfragment separation to the $Na(^2P) + H(^2S)$ atomic limit are the $A\ ^1\Sigma^+$ and $B\ ^1\Pi$ states which carry oscillator strength from the ground state, plus $b\ ^3\Pi$ and $c\ ^3\Sigma^+$ triplet states. The $A\ ^1\Sigma^+$ and $b\ ^3\Pi$ surfaces are the only dissociative molecular surfaces with a stable minimum. In the presence of a repulsive centrifugal potential, a barrier is formed on these surfaces. Long lived complexes (shape resonances) are supported by these two surfaces when the translational energy of the fragments is less than the height of the centrifugal barrier, and the particles must tunnel through the barrier to dissociate. *Ab initio* ABO electronic potential surfaces and transition moments for NaH[10] were used in the calculation. The details of the calculation[11] and some preliminary results[8] are described elsewhere.

The differential cross section for detection of photofragments at angle θ with respect to the polarization vector of incident radiation linearly polarized along the SF z-axis may be written in the form

$$\frac{d\sigma}{d\Omega}(j_{Na}) = \frac{1}{4\pi}\sigma(j_{Na})[1 + \beta(j_{Na})P_2(\cos\theta)] \tag{4.1}$$

where $P_2(\cos\theta)$ is the Legendre polynomial of second order, $\sigma(j_{Na})$ is the total photofragment cross section, and $\beta(j_{Na})$ is the anisotropy parameter which encapsulates all information about the asymmetry of the fragment angular distribution.

The differential cross section for spontaneously emitted photons with polarization vector $\hat{\mathbf{e}}_s$ produced by the decay of excited $Na(^2P)$ fragments to $Na(^2S)$ may be written in the same form as the

photofragment differential cross Section (4.1) given above,

$$\frac{d\sigma_s}{d\Omega}(j_{\mathrm{Na}}) = \frac{1}{4\pi}\sigma_s(j_{\mathrm{Na}})[1+\beta_s(j_{\mathrm{Na}})P_2(\cos\theta_s)] \tag{4.2}$$

where $\hat{\mathbf{e}}_s \cdot \hat{\mathbf{z}} = \cos\theta_s$. Like the photofragment differential cross section (4.1), the above form of the fluorescence differential cross section only applies if the incident radiation is linearly polarized. The polarization ratio (3.2) is given in terms of the anisotropy parameter $\beta_s(j_{\mathrm{Na}})$ for spontaneous emission by a simple formula which is derived by setting θ_s equal to 0 and $\pi/2$ in order to obtain the intensity of fluorescence parallel and perpendicular to the SF z-axis, respectively.

$$P(j_{\mathrm{Na}}) = 3\beta_s(j_{\mathrm{Na}})[4+\beta_s(j_{\mathrm{Na}})]^{-1} \tag{4.3}$$

The total fluorescence cross section $\sigma_s(j_{\mathrm{Na}})$ is related to the fragment cross section $\sigma(j_{\mathrm{Na}})$ by a constant factor, although $\beta(j_{\mathrm{Na}})$ and $\beta_s(j_{\mathrm{Na}})$ vary independently. Fine structure states with total electronic angular momentum less than unity do not emit polarized fluorescence so $\beta_s(j_{\mathrm{Na}}=\frac{1}{2})$ vanishes identically.

Total cross sections for dissociation of NaH from the lowest vibrational level of the $X\ ^1\Sigma^+$ ground state and total initial angular momentum $J_i = 10$ to each of the sodium fine structure states are presented in Figure 2. There is a huge resonance peak at 12 cm^{-1} of excess translational energy in the $\mathrm{Na}(^2P_{1/2})$ cross section but not for the $\mathrm{Na}(^2P_{3/2})$ cross section. No experimental confirmation of interchannel resonances of this type near a dissociation threshold is available at present. (Translational energies are measured from the average energy, or barycenter, of the $\mathrm{Na}(^2P)$ spin–orbit state.) A much smaller and sharper peak is observed in the cross section to both Na fine structure states at 20 cm^{-1} excess translation energy. The resonance peak at 12 cm^{-1} can be associated with the $A\ ^1\Sigma^+$ surface and the peak at 20 cm^{-1} with the $b\ ^3\Pi$ surface.[8] The latter peak would not be observed in our calculations without the inclusion of spin–orbit coupling, yet this peak is the dominant feature of the $\mathrm{Na}(^2P_{3/2})$ cross section near threshold. The resonance associated with the $b\ ^3\Pi$ surface causes dramatic variation of the photofragment angular distribution and fluorescence anisotropy near 20 cm^{-1} (Figure 3).

We have also calculated differential cross sections for photofragments and fluorescence for two-photon, two-color dissociation of

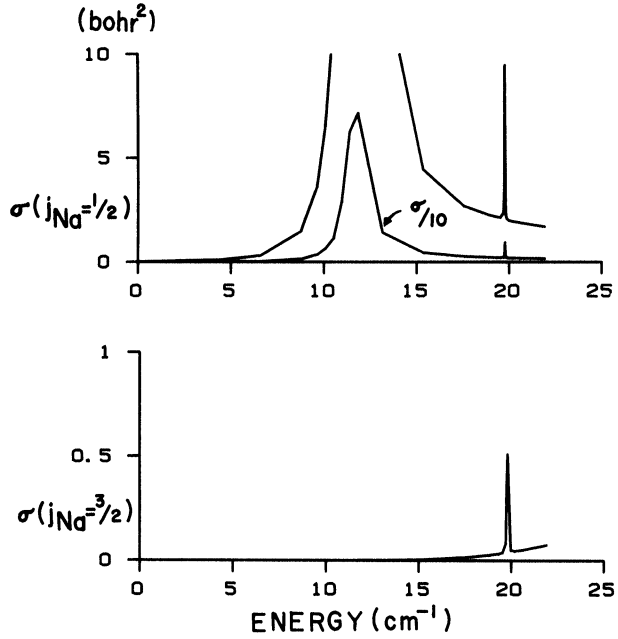

FIGURE 2 Calculated NaH photodissociation cross sections for production of $Na(^2P_{1/2})$ and $Na(^2P_{3/2})$ fragments in the near threshold region. The molecule is dissociated by a single photon from the lowest vibrational level of the $X\ ^1\Sigma^+$ state of NaH with total angular momentum before absorption $J_i = 10$. Energy is measured from the average energy, or barycenter, of the $Na(^2P)$ spin–orbit states.

NaH.[7] The first photon excites the NaH molecule to a particular rovibronic level of the $A\ ^1\Sigma^+$ state. After absorption of the first photon the molecule is prepared in an anisotropic state due to the polarization of the photon. (Even unpolarized excitation would prepare the molecule in an anisotropic state since the propagation vector of the incident radiation defines a unique axis for the system in the SF coordinates.) In contrast to single photon dissociation, the two-photon dissociation occurs from an intermediate state which is already anisotropic. This additional asymmetry is the essential difference between the one and two-photon processes. It is well known that photofragment differential cross sections for two-photon excitation may have multipole components given by Legendre polynomial components up to order 4. The differential photofragment cross section

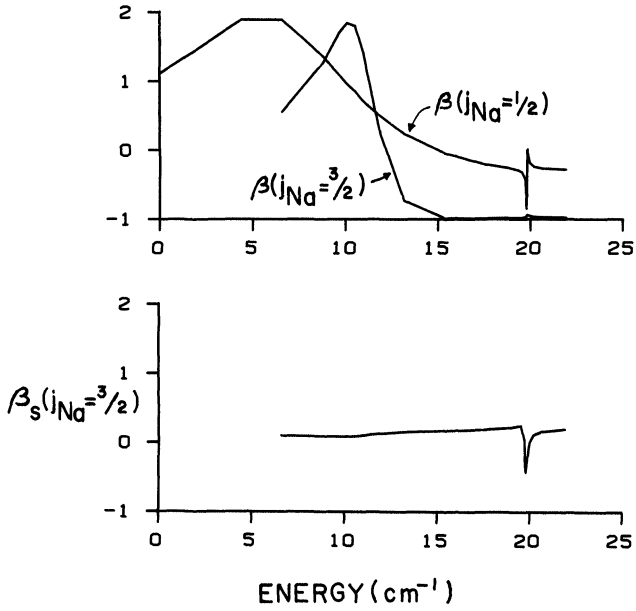

FIGURE 3 Calculated anisotropy parameters for $Na(^2P_{1/2,3/2})$ and $H(^2S_{1/2})$ fragments produced by single photon dissociation of NaH in the near threshold region. The preparation of the NaH molecule before dissociation is the same as that in Figure 2. Energy is measured from the average energy, or barycenter, of the $Na(^2P)$ spin–orbit states. Photofragment anisotropy parameter for $Na(^2P_{1/2})$ and $Na(^2P_{3/2})$ fragments (top graph). Fluorescence anisotropy parameter for $Na(^2P_{3/2})$ fragments (bottom graph).

for two-photon excitation may be written in the following form if both photons are polarized along the SF z-axis.

$$\frac{d\sigma}{d\Omega}(j_{Na}) = \frac{1}{4\pi}\sigma(j_{Na})[1+\beta(j_{Na})P_2(\cos\theta)+\gamma(j_{Na})P_4(\cos\theta)] \qquad (4.4)$$

5. CONCLUSIONS

At fragment translational energies far in excess of the magnitude of non-adiabatic coupling matrix elements, transition amplitudes to atomic fragment eigenstates are given in terms of amplitudes to molecular excited states (Eq. 3.1). When only one molecular excited

state participates in the photodissociation in the recoil limit, the various observable branching ratios and anisotropies may be completely evaluated without consideration of the molecular potential curves themselves and without any further dynamical calculations. When more than one molecular excited state enters into the photodissociation in the recoil limit, then additional dynamic information is required. However, this information involves only the amplitudes for dissociation on single molecular adiabatic states, and these are rather simply evaluated, often from semiclassical methods. Hence, when a single molecular transition contributes in the recoil limit, the experiments can be used to deduce the symmetry of this excited state, whereas the contribution of more than one state gives information concerning the shapes of the potentials themselves. In the latter case experiments can be performed as a function of exciting wavelength to aid in fitting the molecular curves.

When the translational energy of the receding photofragments is small, that is, near a threshold for dissociation, a full dynamical calculation of the transition amplitudes is necessary. In this regime cross sections and asymmetry parameters for each atomic fragment state display strong variations with energy, including resonance structure, which intimately reflect the shape of the excited molecular energy curves, their symmetry, and the non-adiabatic coupling. To our knowledge there is not yet any experimentally confirmed observation of interchannel resonances of the type we calculate for NaH, although some may have been observed for CH^+.[13] Hence, near threshold photodissociation appears to afford excellent opportunities for experimentally determining interatomic potentials between open shell atoms. The traditional approach involving crossed molecular beam scattering is more problematic, especially when one of the fragments is electronically excited and the other is a radical as in the NaH case. Relevant crossed beam experiments that yield information about the potential curves are difficult to perform, and there is an average over initial impact parameters to deconvolute. In contrast, the diatomic dissociation can often be probed at low energies using the monochromaticity of laser excitation. Moreover, with the initial state selection attainable in two-photon excitation, the total angular momentum of the molecule is fixed within one unit prior to dissociation. This leads us to believe that low energy diatomic dissociation will become an important tool for studying intermolecular interactions between

open shell atoms and, in particular, the intermediate and long range attractions which are hard to calculate theoretically and to measure by other techniques. Thus, one of the purposes of our theoretical work is to provide the full quantum mechanical machinery for analyzing such experimental data to its fullest. It is also clear that similar effects will be observed for polyatomic molecules. The theory for dissociation of polyatomic molecules in the presence of non-adiabatic interactions can be built upon the theory presented here for diatomic molecules.

References

1. M. Shapiro and R. Bersohn, *Annu. Rev. Phys. Chem.* **33,** 409 (1982).
2. W. M. Gelbart, *Annu. Rev. Phys. Chem.* **28,** 323 (1977).
3. K. F. Freed and Y. B. Band, in: *Excited States 3*, ed. E. C. Lim (Academic Press, New York, 1977) p. 110.
4. S. R. Leone, *Adv. Chem. Phys.* **50,** 225 (1982).
5. Y. B. Band, K. F. Freed and D. J. Kouri, *Chem. Phys. Lett.* **79,** 233 (1981).
6. Y. B. Band and K. F. Freed, *Chem. Phys. Lett.* **79,** 238 (1981).
7. S. J. Singer, K. F. Freed and Y. B. Band (submitted to *J. Chem. Phys.*).
8. S. J. Singer, K. F. Freed and Y. B. Band, *Chem. Phys. Lett.* **91,** 12 (1982).
9. R. N. Zare, *Mol. Photochem.* **4,** 1 (1972).
10. E. S. Sachs, J. Hinze and N. M. Sabelli, *J. Chem. Phys.* **62,** 3367 (1975).
11. Y. B. Band, K. F. Freed and D. J. Kouri, *J. Chem. Phys.* **74,** 4380 (1981); S. J. Singer, K. F. Freed and Y. B. Band, *J. Chem. Phys.* **77,** 1942 (1982),
12. J. C. Tully, R. S. Berry and B. J. Dalton, *Phys. Rev.* **176,** 95 (1968); M. M. Lambropoulos and R. S. Berry, *Phys. Rev. A.* **8,** 855 (1973); K. Chen and E. S. Yeung, *J. Chem. Phys.* **72,** 4723 (1980).
13. P. C. Cosby, M. Melm and J. T. Moseley, *The Astrophysical Journal* **235,** 52 (1980); A. Carrington, J. Buttenshaw, R. A. Kennedy and T. P. Softley (preprint); H. Helm, P. C. Cosby, M. M. Graff and J. T. Mosely (preprint).